RSC Advances

PAPER

View Article Online
View Journal | View Issue

Cite this: *RSC Adv.*, 2018, **8**, 18272

A smart multi-functional coating based on anti-pathogen micelles tethered with copper nanoparticles *via* a biosynthesis method using L-vitamin C

Yan Li,†[a] Qing-meng Pi,†[cd] Hui-hui You,[e] Jin-quan Li,[f] Peng-cheng Wang,[a] Xu Yang[e] and Yang Wu *[ab]

A multi-functional anti-pathogen coating with "release-killing", "contact-killing" and "anti-adhesion" properties was prepared from biocompatible polymer encapsulated chlorine dioxide (ClO_2) which protected the active ingredient from the outside environment. A slow sustained-release of ClO_2 from micelles over fifteen days was detected for long-term release-killing. Micelles only release ClO_2 on demand in minimum inhibitory concentrations. We prepared nanoparticles which were covalently clustered on micelle surfaces to improve contact-killing as well as to improve the stability of the micelle. Copper nanoparticles were generated using the biosynthesis method including L-vitamin C, which avoids the toxicity and allows for the preparation of copper nanoparticles in a green environment. Synergistic anti-pathogen activity could be generated by a combination of micelle released ClO_2 and ascorbic acid. In addition to release-killing and contact-killing, a pluronic polymer coated surface also provides an additional "anti-adhesion" property through its protein-repelling ability. In this research, the designed coating demonstrated a broad-spectrum of activity to kill drug-resistant bacteria, viruses and spores in short period of time. Based on scanning electron microscopy (SEM), transmission electron microscopy (TEM) and anti-oxidase assays, we found that the designed coatings killed the pathogens *via* bio-oxidation. We also carried out acute respiratory toxicity tests in this research. Analysis of blood samples, lung function and histopathological slices indicated that the synthesized micelles allowed a controlled and sustained release of ClO_2 to kill pathogens while maintaining an overall ClO_2 concentration in the air within a safe range.

Received 6th March 2018
Accepted 13th May 2018

DOI: 10.1039/c8ra01985a

rsc.li/rsc-advances

1. Introduction

The World Health Organization (WHO) recently reported that infectious diseases remain the second leading cause of death.[1] With increasingly frequent international exchanges, and the rapid development of transportation, infectious diseases are emerging and being disseminated faster now than at any time in history. Any one of these cases could trigger a widespread epidemic across the world. Varietal pathogen (*e.g.* H1N1 flu virus) induced epidemics are typical examples in recent years.[2] Epidemiological studies have shown that the transmission route greatly affects the spread of the disease among populations.[3,4] Hand contact with pathogen-contaminated surfaces is regarded as one of the most common routes in promoting transmission of infectious diseases.[5] Research evidence indicates that pathogenic microorganisms can survive from a day to months on surfaces of objects.[6] Some pathogens can even generate a germicide-resistant biofilm if they are not cleaned up in a timely manner.[7,8] Therefore, frequent surface disinfection becomes very important in infectious disease control.

Commercial disinfectants are popular for daily cleaning of household areas and public places. But research has shown that routine disinfection is inadequate for decontaminating pathogen-contaminated surfaces.[9] Nosocomial infections are still common occurrences, even when hospitals do "standard"

[a]*Key Laboratory for Deep Processing of Major Grain and Oil (Wuhan Polytechnic University), Ministry of Education, College of Food Science and Engineering, Wuhan Polytechnic University, Wuhan 430023, P. R. China. E-mail: wuyangwhpu@163.com; Fax: +86-27-83956793 ext. 208; Tel: +86-13871548015*

[b]*Hubei Key Laboratory for Processing and Transformation of Agricultural Products (Wuhan Polytechnic University), College of Food Science and Engineering, Wuhan Polytechnic University, Wuhan 430023, P. R. China*

[c]*Department of Plastic and Reconstructive Surgery, Renji Hospital, Shanghai Jiaotong University School of Medicine, Shanghai 200129, P. R. China*

[d]*Harvard-MIT Division of Health Sciences and Technology, Massachusetts Institute of Technology, Cambridge, MA 02139, USA*

[e]*Hubei Key Laboratory of Genetic Regulation and Integrative Biology, College of Life Sciences, Central China Normal University, Wuhan 430079, P. R. China*

[f]*Brain and Cognitive Dysfunction Research Center, School of Medicine, Wuhan University of Science and Technology, Wuhan 430081, P. R. China*

† These authors contributed equally.

cleaning. This suggests that a sustained "antimicrobial surface" would be of value for controlling the transmission of infectious disease. With the advances being made in material science, the emerging antimicrobial coatings appear to be good candidates for providing a sustained "anti-pathogen surface". For example, modern nanotechnology can generate a coating that can be used to decontaminate a surface by contact-killing. Coatings based on nano-Ag[10] or photocatalytic materials[11] are the most commonly used. However, a relatively long contact time or very specific conditions (for example, the need for UV activation) are technological constraints that limit their use. Storing anti-pathogen agents in bulk materials is another strategy to produce antimicrobial surfaces.[12] The gradual release of a biocide provides a sustained release-killing to a pathogen-contaminated surface. It can rapidly kill pathogens attached to an object's surface. However, controlling the biocide release is a concern with respect to people. Since the overuse of antibiotics is known to promote the development of antibiotic-resistant pathogens,[13] an environmental-response encapsulation system is required to avoid generating unnecessary environmental contamination.

More recently, multiple approaches have been taken to generate new functional coatings that are "smart", environmentally friendly and lethal to pathogens. One approach is to combine release-killing and microbe-repelling. The most prominent example of this is antifouling paint.[14] The paint surface prevents microbe adhesion and kills pathogens.[15] Another approach is to enhance the activity of the antimicrobial surface by combining release-killing with an active contact-killing approach. For example, Li *et al.* produced a dual-function coating having a very high initial bacteria-killing efficiency due to the release of Ag ions, while immobilized quaternary ammonium salts in the coating provided significant antibacterial activity *via* the surface, even after depletion of the embedded Ag.[16] Rivero *et al.* prepared a similar coating which was based on surface tethered bactericides and Ag release-killing.[17] The combination of contact-killing and repelling is also widely used in the production of antimicrobial coatings. For example, Chen *et al.* created an antimicrobial contact-active surface to kill, and effectively repel, all attached microbial cells.[18] Laloyaux *et al.* produced polymer brushes of attached magainin grafted with oligo(ethylene glycol) methacrylates to kill microbial cells. The coating surface repelled microbes when heated above 35 °C.[19]

In our work, we synthesized a smart, multi-functional anti-pathogen coating. This coating provides long-term antimicrobial performance by combining release-killing, contact-killing, and anti-adhesion properties. ClO_2 is an approved safe agent used against a broad spectrum of bacteria, viruses, protozoa, and even bacterial spores over a wide pH range (pH 2–8).[20] Both pluronic P123 (P123) and pluronic F127 (F127) were used to generate micelles to encapsulate ClO_2, and these complexes then could be used for controlled release-killing. Micelles only release ClO_2 on demand at minimum inhibitory concentrations. These polymers have been approved by the US Food and Drug Administration (USFDA) and United States Environmental Protection Agency (USEPA). They have excellent biocompatibility and biodegradability. This strategy can effectively increase the service life of ClO_2 through reducing unwanted evaporation. The polymer-coated surface provides additional anti-adhesion efficiency due to their ability to easily repel proteins.[21–23] A mixture of ascorbic acid and copper was added to provide an additional contact-killing property. Because L-ascorbic acid (L-vitamin C) mixed with copper could generates nanoscale copper and free radicals, which is known to effectively kill pathogens even at the ppm level.[24] These bio-friendly components greatly increase the environmental friendliness of designed coatings. In this research, anti-pathogen assays of the designed coating were performed to bacteria, spore, virus and drug resistant bacteria. We also studied the biomechanisms and biosafety of the designed coating in this work. The objective being to measure the broad-spectrum anti-pathogen activity and to gain a better understanding of this multi-functional antimicrobial coating (Fig. 1).

2. Results and discussion

2.1. Multi-functional anti-pathogen formulation

The ClO_2 biocide was encapsulated by polymers of P123 and F127 in a w/o/w double emulsion. These polymers are from the pluronic family of polyoxyethylene–polyoxypropylene triblock copolymers which are safe and widely studied for use in medicine as well as in cosmetics. The preparation procedure followed the basic procedure described by Ficheux and Li.[25,26] ClO_2 was first encapsulated with a low hydrophilic-lipophilic balance (HLB) polymer (P123) which was dissolved in essential oil to generate a w/o emulsion. P123 ($EO_{20}PO_{70}EO_{20}$) is an amphiphilic copolymer and is composed of a central hydrophobic chain of polyoxypropylene (poly(propylene oxide)) [PPO] flanked by two hydrophilic chains of polyoxyethylene (poly(ethylene oxide)) [PEO]. The hydrophilic head of P123 can be linked with ClO_2 water molecule as well as hydrophobic head linked with oil to form w/o emulsion. The emulsion was then emulsified again with a high HLB polymer (F127) to produce a w/o/w double emulsion. Finally, a mixture of copper chloride and ascorbic acid was added. In this research we characterized the prepared anti-pathogen formulation and coatings. Double emulsions measuring 10–20 microns in diameter were predominant in the one month old sample (Fig. 2A). It is possible to see the smaller micrometer-sized w/o emulsion within the capsules. The synthesized double emulsion was a vesicular system where small waterphase droplets (internal aqueous phase) were entrapped within larger oil droplets (oil phase) that in turn are dispersed in a continuous water phase (external aqueous phase) (Fig. 2A).

Based on UV-vis analysis, the ClO_2 characteristic peak is shown in either the polymer encapsulated ClO_2, or in the anti-pathogen coating (Fig. 2C). Results demonstrated that applied polymers should not be oxidized by ClO_2 and resulting in instability and phase separation. Copper/ascorbic acid does not induce instability in the ClO_2 molecule either. Images of the anti-pathogen coating further proved these results (Fig. 2B), that is that coatings maintained intact emulsion features.

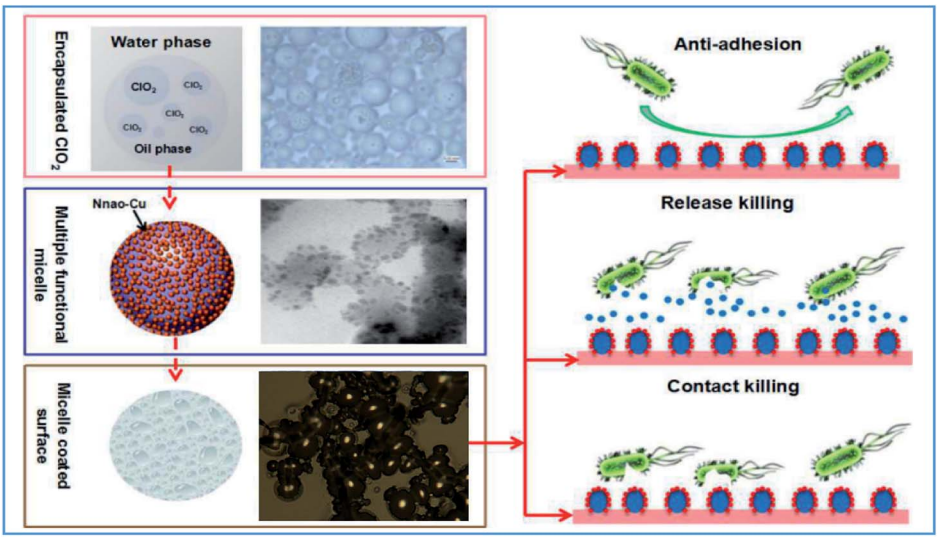

Fig. 1 Scheme of multi-functional anti-pathogen coating.

2.2. Copper nanoparticles tethered to the micelle surface

To avoid toxicity, and to prepare copper nanoparticles in a green environment, we have used ascorbic acid (Vitamin C) in our chemical reduction process. Ascorbic acid works both as a reducing and protecting agent, which makes the process economical, nontoxic and environmentally friendly.[27] Biosynthesis of copper nanoparticles using ascorbic acid was used here for contact-killing.[28] This technique was employed to prepare highly stable and dispersed copper nanoparticles using L-ascorbic acid (Vitamin C).[29] In this research, bulk size cupric chloride (Fig. 3B and 3D) was used as the precursor to the generated nanoscale particles. A TEM image showed that copper nanoparticles were generated and tethered to the micelle surface (Fig. 3A). Energy dispersive spectroscopy (EDS) analysis further proved this result (Fig. 3C). In addition to providing contact-killing, copper nanoparticles are also proposed to increase the stability of anti-pathogen micelles. Based on previous research, the nanoparticles covalently clustered on micelle surfaces could improve the stability of micelles

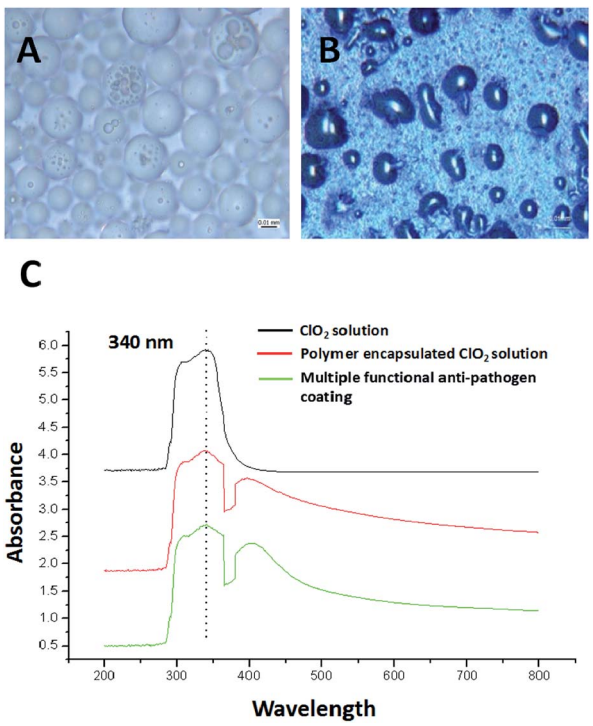

Fig. 2 Characterization of the multi-functional anti-pathogen formulation. (A) Optical microscope picture of anti-pathogen micelles; (B) optical microscope picture of the multi-functional anti-pathogen coating; (C) UV-vis spectroscopy of ClO_2 solution, polymer encapsulated ClO_2 and multi-functional anti-pathogen coating.

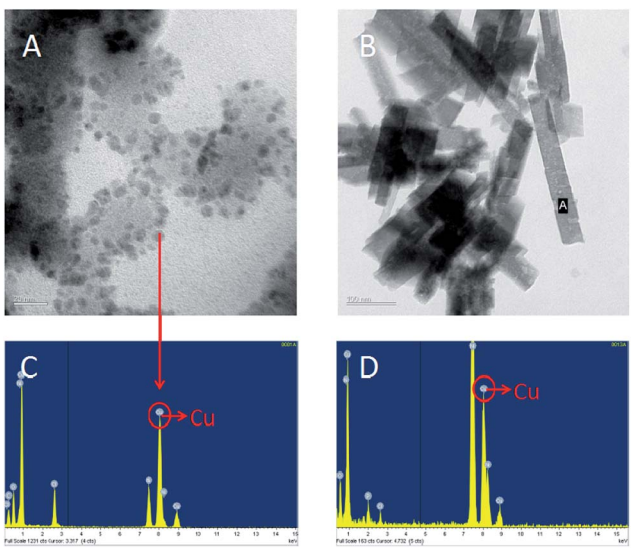

Fig. 3 Transmission electron microscope image of (A) multi-functional anti-pathogen micelles and (B) bulk size of copper chloride; EDS spectrum of (C) copper nanoparticles tethered on the micelle surface and (D) bulk size of copper chloride.

prepared from pluronic triblock copolymers.[30–32] In this research, the fine structures of the prepared micelles were observed by TEM (Fig. 3A). The image suggests that the tethered copper nanoparticles improved the stability of the prepared micelles. The size discrepancy of the micelles between optical microscope and TEM analysis may be due to desiccation at high vacuum conditions for TEM samples.

2.3. Multi-functional anti-pathogen coating exhibits release-killing *via* ClO_2 controlled release

The controlled release of ClO_2 from the multi-functional coating at room temperature was monitored for fifteen days. The coatings were placed in constant-temperature ovens at 60–80% RH. The ClO_2 content within coatings was measured by titration at fixed time intervals. Results showed that approximately 40% of the stored ClO_2 was gradually released over the fifteen days (Fig. 4A), demonstrating that the designed micelles enabled a slow and sustained release of ClO_2. Previous research has reported that water molecules, electrolytes and non-electrolyte, water-soluble substances can easily migrate through an oil membrane without affecting the stability of the double emulsion.[33] According to this theory, the ClO_2 released from the coating may be transported from the interior to the exterior *via* diffusion. Consequently, the ClO_2 is sustainably released from the micelles driven by a mismatch between the osmotic pressures in the interior and the exterior. In addition, the use of polymer (P123) instead of the usual hydrophobic surfactant could eliminate the faster transport route *via* inverted micelles in the oil phase.[34] These properties enable a slow and sustained release of ClO_2. An inhibition zone assay was carried out to further verify the efficiency of release-killing of the anti-pathogen coatings. In this assay, *E. coli* (G^-), *Pseudomonas* (G^-), *B. subtilis* (G^+) and *S. aureus* (G^+) were investigated. The inhibition zone is simply the area on the agar plate that remains free from microbial growth. As compared to the negative control (DDI water) or the positive control (75% ethanol), the average zone diameters of the anti-pathogen coating are 4.1 cm (*E. coli*), 3.7 cm (*Pseudomonas*), 3.3 cm (*S. aureus*) and 3.5 cm (*B. subtilis*). The anti-pathogen coating exhibited a great release-killing efficiency against the tested pathogens (Fig. 4B).

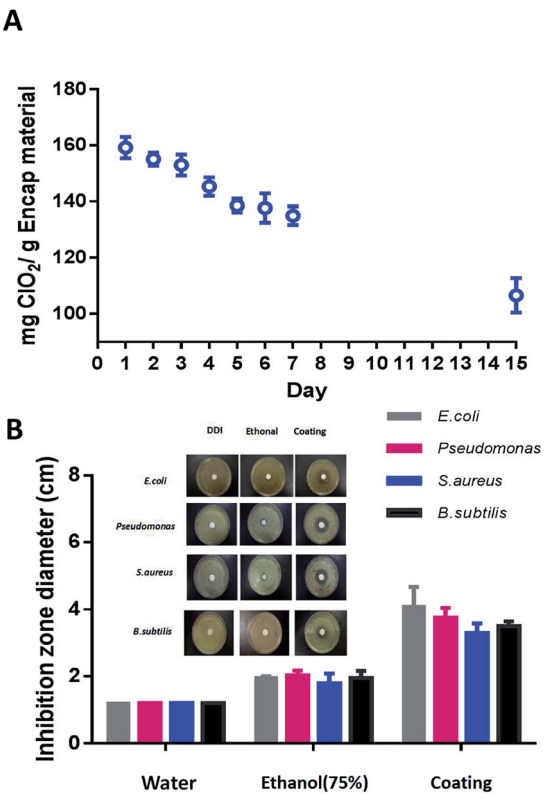

Fig. 4 Multi-functional anti-pathogen coating exhibits release-killing *via* the controlled release of ClO_2. (A) Residual ClO_2 within the coating during the 15 day release experiment at ambient temperature (20–26 °C) and humidity (RH = 60–90%); (B) release-killing efficiency of anti-pathogen coating *via* inhibition zone assay.

2.4. Anti-adhesion property of multi-functional anti-pathogen coating

Bacteria can form biofilms which can diminish the effectiveness of antimicrobial coatings.[35] Phenotypic tolerance to oxidizing biocide can arise from biofilm growth as a result of biocide consumption by the organic constituents of the biofilm, and by a "population-based" resistance strategy.[36] The formation of a biofilm begins with the attachment of free-floating microorganisms to a surface. Therefore, an effective anti-adhesion property is useful for antimicrobial efficiency of designed coatings. Pluronic polymers are considered to have anti-adhesive properties against microorganisms.[37] In this research, the pluronic polymers (P123 and F127), were used to encapsulate sterile water in a double emulsion, which is order to verify their anti-adhesion property. Water-containing emulsion micelles were prepared using the same procedure of for the anti-pathogen formulation, but replacing the biocides with distilled water. One hundred microliters of this prepared formulation were coated onto glass. Pathogens (*E. coli* and *S. aureus*) were applied to the coatings and incubated at 37 °C for three days with humidity. As shown in Fig. 5, few pathogens (*E. coli* or *S. aureus*) adhered to the coating surface (Fig. 5A and C) as compared to the uncoated glass (Fig. 5B and D). This result indicates that our applied pluronic polymers are useful in preventing the adhesion of bacteria. In addition, fluorescent *E. coli* formed biofilms on the uncoated glass after 7 days (Fig. 5E). As shown, the designed coating effectively prevented *E. coli* attachment (Fig. 5F), suggesting that the designed multi-functional coating can be used to prevent the formation of bacterial biofilms. Hydrophilic PEO side-chains are considered to promote the anti-adhesion property. This is because water is attracted to the hydrophilic PEO layer and forms a repellent layer close to the surface thus providing an anti-adhesion surface.[38,39] In addition to PEO side-chains, surface tethered copper nanoparticles may also provide additional antibiofilm property. The nano-textured morphology could reduce protein adsorption which inhibit bacterial attachment.[40,41] Nanomaterials are benefit to inhibit biofilm

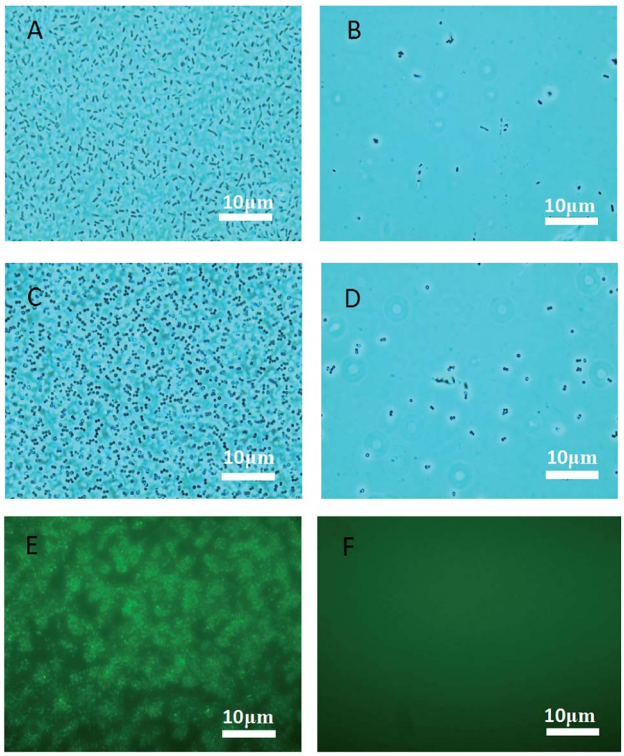

Fig. 5 Anti-adhesion properties of the multi-functional coating. (A) Optical image of *E. coli* adhered to glass after 3 days; (B) optical image of *E. coli* adhered to coating (polymers of P123 and F127 were used to encapsulate sterile water in a double emulsion) for 3 days; (C) optical image of *S. aureus* adhered to glass after 3 days; (D) optical image of *S. aureus* adhered to coating (polymers of P123 and F127 were used to encapsulate sterile water in a double emulsion) after 3 days; (E) optical image of *E. coli* adhered to glass after 7 days; (F) optical image of *E. coli* adhered to coating (polymers of P123 and F127 were used to encapsulate sterile water in a double emulsion) after 7 days.

formation may due to their high surface area to volume ratio and unique chemical and physical properties.[42]

2.5. Bactericidal performance of multi-functional anti-pathogen coating *via* contact-killing

Antimicrobial resistance is an increasingly serious threat to global public health, requiring action across all government sectors and society. With the rapid overuse of antibiotics, microbes have become stronger and less responsive to antibiotic treatment.[43,44] In this research, two drug-resistant pathogens (MRSA and *Acinetobacter baumannii*) were tested to evaluate the contact-killing ability of the multi-functional coating. As shown in Fig. 6, over 99.9% of antimicrobial activity occurred in five minutes of contact time for both pathogens in first five days. The killing performances declined in the following days, but overall antimicrobial activities were still over 99% in the remaining twelve days (Fig. 6A). Based on the above results, the designed coating is supposed to perform contact-killing *via* ClO_2, tethered copper nanoparticles and ascorbic acid. Many studies report that the interaction of ascorbic acid with antibiotics is clinically more effective in inhibiting antibiotic-resistant bacteria.[45,46] ClO_2 is a very reactive biocide that attacks multiple targets in the cell including the cell membrane. When in

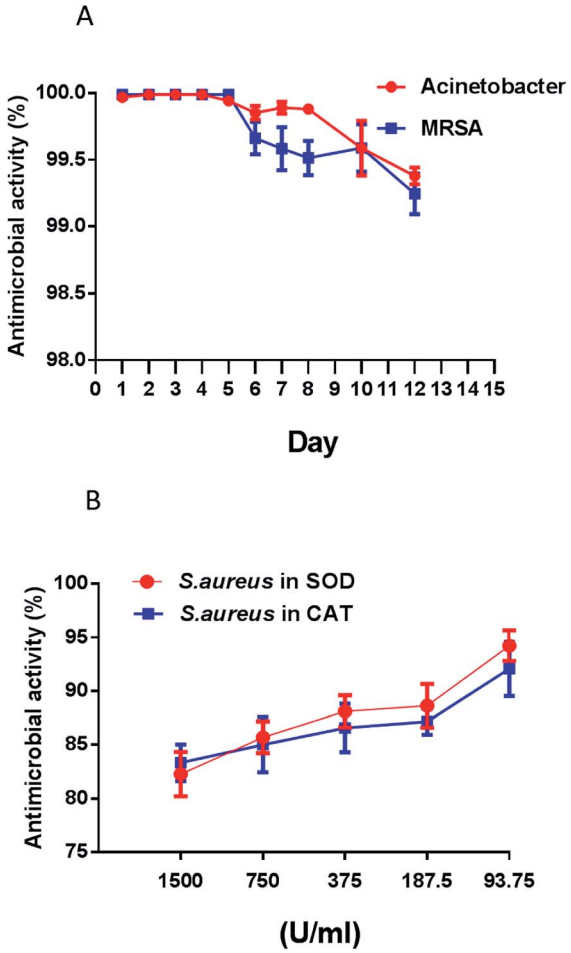

Fig. 6 Contact-killing capability of the multi-functional anti-pathogen coating. (A) Long term antimicrobial performance of the coating surface against MRSA and *Acinetobacter baumannii*; (B) Antimicrobial performance of the coating surface against *S. aureus* containing antioxidase (SOD and CAT).

contact with bacteria, ClO_2 oxidizes the cell membrane and penetrates into the cell to oxidize macromolecules.[47] In addition, in the presence of ascorbic acid and an oxidizing agent, copper is especially active in generating hydroxyl radicals under aerobic conditions. Hydroxyl radicals, a type of reactive oxygen species, are very effective in damaging microorganisms.[48,49]

E. coli (G^-) and *S. aureus* (G^+) are the model bacteria. To further elucidate the antimicrobial mechanisms of the designed coating, we used SEM to observe any morphological changes in these two bacteria after they had come in contact with the coatings. As compared to the control (wavy and smooth cell surface), SEM demonstrated that the designed coating caused extreme damage to the *E. coli* membrane after contact (Fig. 7A and 7B). Unlike *E. coli*, most of *S. aureus* remained intact, however the membranes shrank after contact with the coatings (Fig. 7C and D). The difference can be attributed to Gram-positive bacteria (*e.g. S. aureus*) having thicker cell walls that resist chemical oxidation as compared to Gram-negative bacteria (*e.g. E. coli*). TEM observation was further applied for long term anti-pathogen efficiency against *S. aureus* in 15 days later. As shown in Fig. 7E, fine structures of the prepared

micelles were still be observed by TEM in 15 days later. It means the designed micelles were still hold with well stability within long period. As compare to *S. aureus* control (Fig. 7G and H), anti-pathogen micelles attached to the surface of *S. aureus* to perform the antimicrobial capability (Fig. 7F). Both ClO_2 and hydroxyl radicals can permeate a cell wall and oxidize intracellular biomacromolecules. An antioxidant assay was carried out to prove this hypothesis. An antioxidase is a molecule that inhibits the oxidation of other molecules.[50] Superoxide dismutases (SOD) and catalases (CAT) are very important enzymes in protecting the cell from oxidative damage.[51,52] In this research, antioxidases were mixed with *S. aureus* prior to contact with the coatings. As shown in Fig. 6B, the results clearly demonstrate that antimicrobial performance is inversely proportional to the concentration of antioxidase. Antioxidases (SOD and CAT) effectively promote the viability of *S. aureus* after contact with the surface of the coating. Taken together, the above results lead us to conclude that bio-oxidation contributes to the antimicrobial capability of the designed coating.

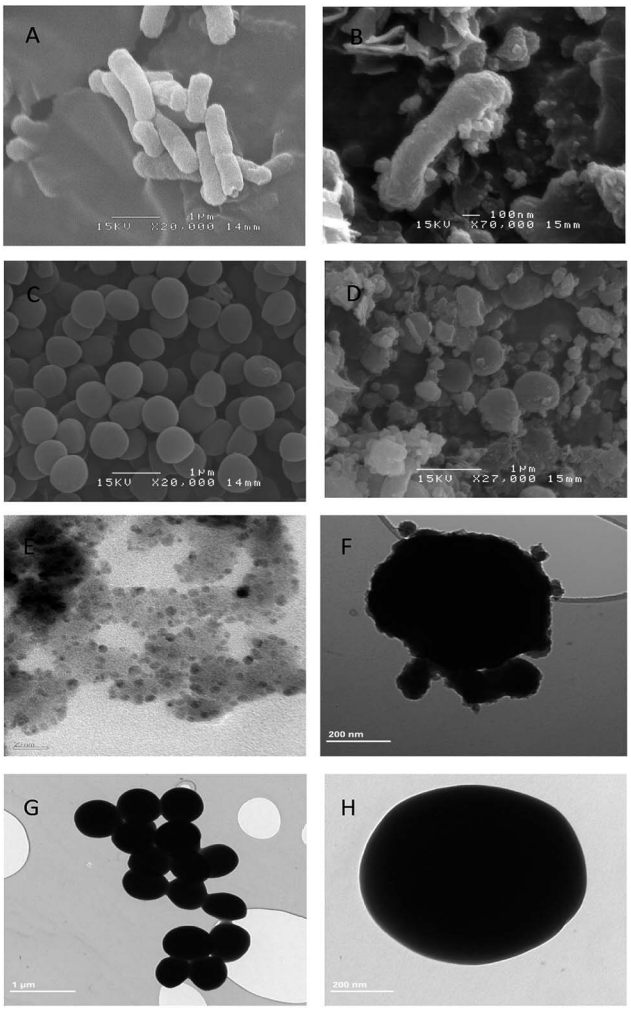

Fig. 7 Scanning electron microscope images of bacterial morphology change: (A) *E. coli* on uncoated glass; (B) *E. coli* contact with multiple functional anti-pathogen coating; (C) *S. aureus* on uncoated glass; (D) *S. aureus* contact with multiple functional anti-pathogen coating. Transmission electron microscope images: (E) anti-pathogen formulation (15 days after preparation); (F) anti-pathogen micelles attached to the surface of *S. aureus* to perform the antimicrobial capability (15 days after preparation); (G–H) *S. aureus* on uncoated glass.

2.6. Sporicidal performance of the multi-functional anti-pathogen coating

Bacterial endospores are considered to be a big threat to public health. Endospores can survive for years without nutrients, and later germinate to resume the vegetative form on encountering a favorable environment. Endospores are also exceptional resistant to heat, radiation and chemicals.[53] In this research, *Cladosporium* spores and *B. subtilis* spores (Fig. 8A and 8C) were tested to investigate the sporicidal activity of the designed coating. As shown in Fig. 8E, the designed coating surfaces exhibited great sporicidal activity within two hours. SEM further demonstrated that the endospore's exosporium was extremely damaged after being in contact with the coating surface (Fig. 8B and D). The exosporium is the most protective part of the entire sport, and is capable of protecting the spore from external attack. If it collapses or is damaged, all the spore's content will leak out and the spore cannot survive. In the designed coating, the micelle-released ClO_2 is an oxidizing agent which has been shown to kill spores.[54] Sporecoats are probably disrupted by this oxidizing sporicidal agent, which facilitates the penetration of ClO_2 into the cortex and protoplast. Micelle tethered copper is also supposed to exhibit sporicidal ability. Research has shown that

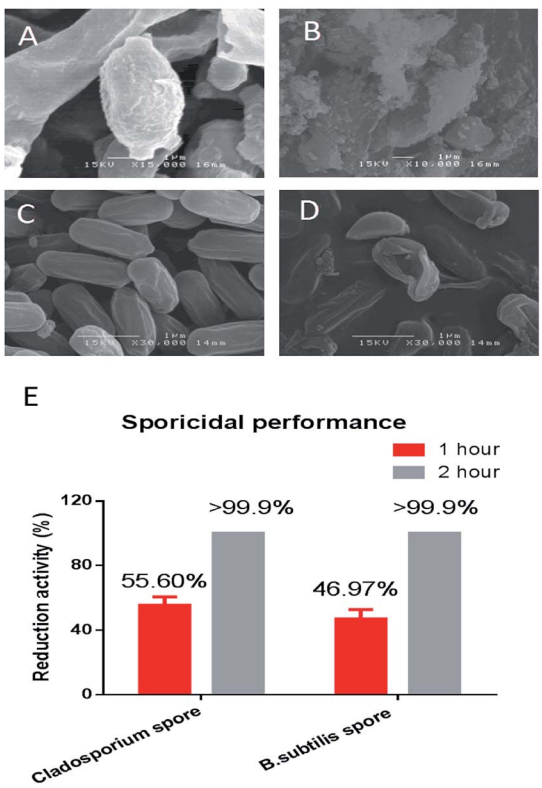

Fig. 8 Sporicidal performance of the multi-functional anti-pathogen coating. (A) SEM image of *Cladosporium* spores; (B) SEM image of *Cladosporium* spores after contact with the coating; (C) SEM image of *B. subtilis* spores; (D) SEM images of *B. subtilis* spores after contact with the coating; (E) virucidal activity of coating.

copper is especially effective for killing spores in the presence of ascorbic acid. The mixture of copper and ascorbic acid could generate hydroxyl radicals which has been proven to kill spores effectively.[55] The synergistic interaction of copper nanoparticles and ascorbic acid provides enhanced contact-killing activity due to bio-oxidation. Ascorbic acid is essential in human tissues, and it is an important antioxidant which is widely used as a food additive and preservative. In addition to its use as an anti-pathogen, we also have used ascorbic acid (Vitamin C) in our chemical reduction process. Ascorbic acid works both as a reducing and protecting agent, and can avoid toxicity when preparing copper nanoparticles in a green environment.

2.7. Virucidal performance of the multi-functional anti-pathogen coating

A virus is a small infectious microorganism that is much smaller than a fungus or bacterium. Numerous viruses of human or animal origin can spread in the environment and infect people *via* air, water or occasionally through skin contact.[56] In addition to causing infectious disease, viruses can also cause explosive epidemics infecting millions of people. For example, an influenza pandemic is an epidemic of an influenza virus that spreads worldwide and infects a large proportion of the world's population. In this research, the designed coating exhibited release-killing by the polymer encapsulated ClO_2, and contact-killing by micelle tethered copper nanoparticles. ClO_2 has a broad spectrum of antimicrobial activity against pathogens including viruses.[57] Copper has also been reported to be an effective product to inactivate a virus.[58] The virucidal activity of copper is increased in the presence of ascorbic acid.[59,60] Based on a viral plaque assay, we tested the coating's virucidal efficiency against the influenza A (H1N1) virus. Plaque assays are the standard method by which viral activity and concentration are determined. As shown in Fig. 9C, an infectious H1N1 virus can infect the host cell and form a virus plaque. Virucidal activity was determined by calculation of plaque numbers. As shown in Fig. 9D, the designed coating deactivated all the H1N1 virus within 1 min. No virus plaque was observed in the host cell monolayer. The H1N1 virus is an enveloped RNA virus. The viral envelope covers its protective protein capsids. As shown in Fig. 9A, the H1N1 virus is a spherical particle with a diameter of 99 nm. The protein envelop was damaged within 1 min after coming into contact with the multi-functional coating (Fig. 9B). Oxidative based damage is still considered to be the possible mechanism for this virucidal performance. ClO_2 mediated deactivation of the influenza virus is due to oxidation, and elimination of the function of the haemagglutinin molecule.[61] Copper also results in deactivation, and this deactivation is enhanced when mixed with ascorbic acid.[62] The designed formulation might be useful in the development of anti-virus coatings.

2.8. Respiratory safety of the multi-functional anti-pathogen coating

As shown above, our designed coating efficiently release-killed *via* ClO_2 controlled release. However, aqueous ClO_2 easily vaporizes and exists as a gas at room temperature.

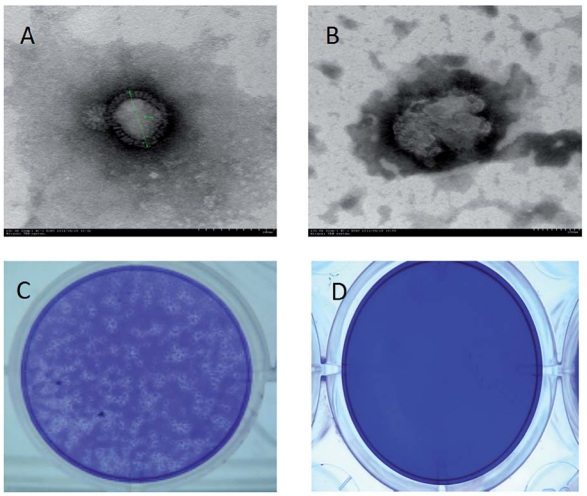

Fig. 9 Virucidal performance of the multi-functional anti-pathogen coating. (A) TEM image of the H1N1 virus; (B) TEM image of the H1N1 virus after contact with the coating; (C) plaque assay image of an H1N1 infected host cell; (D) plaque assay image of the coating inactivated N1N1 virus.

Gaseous ClO_2 is a potent antimicrobial agent,[63–65] but gaseous ClO_2 is also a severe respiratory irritant.[66,67] Countries around the world have set stringent standards for ClO_2 exposure. We therefore evaluated the respiratory safety of the coating-released ClO_2 in this research. Several biomarkers were measured to verify the respiratory safety of the designed coating. First, we analyzed blood leukocyte numbers and bronchoalveolar lavage fluid from mice. Both of these are important indicators of volatile-chemical induced disease.[68] Results demonstrated that the coating released ClO_2 induced no significant increase in the number of leukocytes as compare to clean air (Fig. 10A and 10D). Gaseous formaldehyde (FA) did significantly increase general leukocyte numbers. In addition, we looked at the numbers of neutrophils and lymphocytes. Neutrophils are the most abundant type of leukocyte in mammals, and form an essential part of the innate immune system. A lymphocyte is another type of leukocyte which participates in, and regulates acquired immunity.[69] Our results demonstrated that the number of neutrophils and lymphocytes were increased in the formaldehyde (FA) group while there was no significant increase in the coating group as compare to control (Fig. 10B and C; Fig. 10E and F).

The forced vital capacity (FVC) and force expiratory volume (FEV) as a percentage of FVC (FEV/FVC) are indicators of acute respiratory failure (ARF).[70] They represent the proportion of a person's vital capacity that they are able to expire in a certain time.[71] When compared to the clean air (control), the coating released ClO_2 induced no obvious differences in both the FVC and $FEV_{0.2}$/FVC. The values of FVC and $FEV_{0.2}$/FVC were both reduced by FA (Fig. 11A and 11B). H&E histological staining further support the results as described above. H&E staining is a classical staining method for visualizing airway remodeling, revealing typical pathological features of airway inflammation and structural alterations, including leukocyte infiltration in

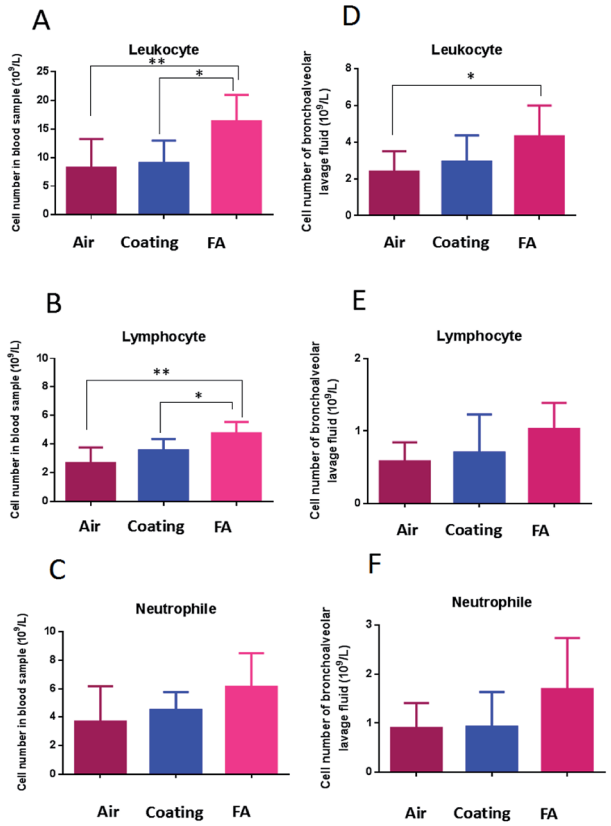

Fig. 10 Respiratory safety of the multi-functional anti-pathogen coating. The number of (A) leukocytes, (B) lymphocytes and (C) neutrophiles in the blood; the number of (D) leukocytes, (E) lymphocytes and (F) neutrophiles in bronchoalveolar lavage (*P < 0.05, **P < 0.01).

surrounding peribronchiolar areas, epithelial folding, and thickened subepithelial cell layers. The H&E stained slides showed normal airway histology for the clean-air and designed-coating groups (Fig. 11C and D). But formaldehyde was seen to induce pathological changes including epithelial folding and thickened subepithelial cell layers (Fig. 11E). Based on these results, we concluded that the designed multi-functional coating has good respiratory biocompatibility. The elevated ClO_2 concentration at the surface ensured high effectiveness against most microorganisms, yet the overall ClO_2 concentration in the air is maintained in a safe range for long-term exposure in the workplace.

3. Methods

3.1. Preparation of the multi-functional anti-pathogen formulation

On the basis of previous studies of polymeric micelle preparation,[72,73] we make a suitable modification and prepared the multi-functional anti-pathogen formulation. The stabilized ClO_2 aqueous solution (United Laboratories Ltd) was encapsulated in triblock copolymers of polyoxyethylene–polyoxypropylene (P123 and F127, BASF Corp, USA) using a water-in-oil-in-water (w/o/w) emulsion method. Briefly, a monodisperse water-in-oil emulsion (w_1/o) was prepared and stabilized by

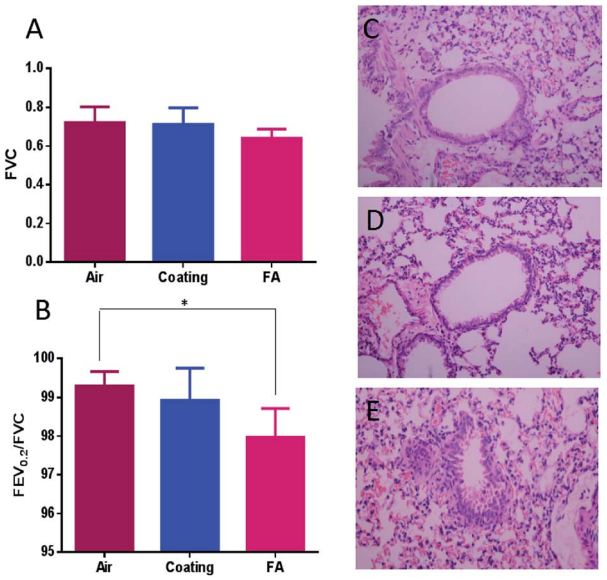

Fig. 11 Lung function measurement *via* (A) forced vital capacity (air, anti-pathogen coating, formaldehyde) and (B) $FEV_{0.2}$/FVC (air, anti-pathogen coating, formaldehyde); H&E staining of mouse airway tissue after exposure to (C) clean air, (D) the anti-pathogen coating and (E) formaldehyde (*P < 0.05).

an oil-soluble surfactant. Twenty-five milliliters of activated 5% (v/v) ClO_2 were suspended in the lemon oil (1 ml, Sigma-Aldrich) and 25 ml of 5% (w/v) Pluronic P123 ($EO_{20}PO_{70}EO_{20}$, MW 5750 g mol^{-1}) surfactant solution. The emulsion was obtained by incorporating the dispersed phase with very gentle stirring (*i.e.*, 400 rpm). The w_1/o primary emulsion was then re-emulsified in aqueous solutions of 5% (w/v) Pluronic F127 ($EO_{106}PO_{70}EO_{106}$, MW 12600 g mol^{-1}) at 400 rpm (10 min) to generate the double emulsion. Finally, the ascorbic acid/copper mixture was added to the prepared double emulsion (ascorbic acid = 100 ppm; copper chloride = 30 ppm).

3.2. Characterization of the multi-functional anti-pathogen coating

The prepared anti-pathogen coatings were characterized by optical microscope (Olympus-BX53) and transmission electron microscopy (TEM, JEOL JEM-2010F) at 200 kV. ClO_2 release from the designed coating was measured at different times to monitor the release of ClO_2. Briefly, 100 μl of the prepared anti-pathogen formulation were coated onto glass (2.5 × 2.5 cm^2). The coated glass was sonicated in 20 ml of deionized distilled water to dissolve the coatings. An excess amount of potassium iodide (KI, BDH) was added, and iodometric titration was carried out in an acidic medium. The free iodine (I_2) was titrated with 0.1 M sodium thiosulfate ($Na_2S_2O_3$, RDH) with starch indicator.

3.3. Bactericidal properties of multi-functional anti-pathogen coating

B. subtilis (ATCC 21332); *E. coli* K12 (ATCC® 10798™); *S. aureus* (ATCC® 25923™); *Pseudomonas aeruginosa* (ATCC® 27853™);

methicillin-resistant *Staphylococcus aureus* (ATCC® MP-3™) and *Acinetobacter baumannii* (BAA-1605™) were tested in this research. The bactericidal tests were performed using a set of standard operating procedures according to the Association of Official Analytical Chemists (AOAC International). One hundred microliters of prepared anti-pathogen formulation was coated onto glass (2.5×2.5 cm^2). All tested bacteria were cultured in nutrient broth. The nutrient broth was removed from cultured bacteria by centrifugation. The precipitated bacteria were resuspended with PBS. A hundred microliters of bacteria cell suspension (10^6 cells per ml) was placed in contact with the coated glass at ambient temperature (23 ± 2 °C) in a sterilized biological safety cabinet (NuAire, Nu-425-400E) for 5 minutes. Then samples were immersed in a primary subculture tube containing 20 ml neutralizer and vortexed to recover the surviving bacteria cells. The sterile neutralizer solution was freshly prepared by adding 1% (v/v) 0.1 M $Na_2S_2O_3$ to 600 ml of 0.85% (w/v) normal saline (NaCl, RDH) solution containing 0.1% (v/v) (final concentration) of polyoxyethylenesorbitan monooleate (Tween 80) followed by autoclaving at 121 °C for 20 min. One hundred microliters aliquots from the neutralizer were cultured on a tryptone soya agar (TSA) plate. The numbers of viable bacterial colonies were counted after incubating the plates for 24 h at 37 ± 0.1 °C.

3.4. Inhibition zone test

Four kinds of bacteria (*B. subtilis*; *E. coli* K12; *S. aureus*; *Pseudomonas aeruginosa*) were tested in this research. All tested bacteria were cultured in nutrient broth. The nutrient broth was removed from cultured bacteria by centrifugation. The precipitated bacteria were resuspended with PBS. Briefly, 40 μl of new cultured bacterial suspension (10^6 cell per ml) were uniformly spread on TSA agar plate. Filter paper (diameter, 15 mm) was coated with 100 μl of prepared anti-pathogen formulation. The coated filter papers were transferred to the center of the agar plate and kept in the dark at room temperature. Inhibition zone diameters were measured after three days. Filter papers coated with sterilized water and ethanol were used as a negative control and a positive control respectively.

3.5. Anti-adhesion properties of multi-functional anti-pathogen coating

Distilled water was encapsulated by P123 and F127, which were prepared using the same procedure as described in Section 2.1. One hundred microliters of prepared formulation were coated on glass (uncoated glass was used as the control). One hundred microliters of *E. coli* or *S. aureus* (10^9 cell per ml) suspension were uniformly spread on the coated or uncoated glass surfaces. Samples were incubated at 37 °C without shaking. The samples were gently washed with sterile distilled water to remove any non-adhered bacteria. The washed glass was examined under a microscope (Nikon, Eclipse TS 100, Japan) to quantify the degree of bacterias adhesion on the coated and uncoated surfaces.

3.6. Sporicidal properties of multi-functional anti-pathogen coating

B. subtilis endospores (Carolina 15-4921A) and *Cladosporium* spores (ATCC® 11275™) were tested in this research. One hundred microliters of spore suspension (10^5 cell per ml) was placed on the surface of the multi-functional coating under ambient conditions (23 ± 2 °C) in a sterilized biological safety cabinet (NuAire, Nu-425-400E). Sporicidal activity of the designed anti-pathogen coatings was measured for a contact time of 60 min or 120 min. After the required contact time, the substrates were immersed in 20 ml neutralizer for 30 min to stabilize the surviving spores followed by 20 ml of nutrient broth for 10 min. The numbers of viable spores were determined by counting the number of viable bacteria colonies on the plates. One hundred microliter aliquots from the neutralizer were cultured on agar plates. The numbers of viable spores were calculated by counting the viable bacteria colonies on the plates after incubation for 24 h at 37 ± 0.1 °C.

3.7. Virucidal properties of the multi-functional coating

Virucidal measurements was carried out for the influenza virus (H1N1) (ATCC ® VR-95™). Ten microliters of virus solution (10^5 pfu ml^{-1}) was deposited in the center of the prepared anti-pathogen coatings. A plain glass slide was placed on top and pressed to obtain a uniform spread of the virus solution. The virus was allowed to remain in contact with the sample at room temperature for 1 minute, which is to ensure deactivation of the influenza virus. The sample and the glass slides were washed with neutralizer. The negative control was an uncoated glass slide. A plaque assay to determine the virucidal activity was performed according to the method previously described by Gaush *et al.*[74] The influenza A (H1N1) virus was deactivated before morphology observation using transmission electron microscopy (TEM) (JEM JEOL 2010F).

3.8. Biosample preparation for SEM and TEM

Pathogens were placed in contact with the multi-functional anti-pathogen coating. Uncoated glass was used for the control. Samples were washed by neutralizer and collected by centrifuge at 8000 rpm for 10 min. Deposits were fixed with 2.5% glutaraldehyde in cacodylate buffer (0.1 M sodium cacodylate–HCl buffer pH 7.4, Sigma-Aldrich) for 4 to 24 hours at 4–8 °C. Samples were washed in cacodylate buffer (Sigma-Aldrich) with 0.1 M sucrose to remove excess fixative solution. Finally, samples were dehydrated with an increasing series of ethanol concentrations (99.9%, Sigma-Aldrich) of 30%, 50%, 70%, 90% and 100%. Dehydrated samples were dried in a Critical Point Dryer before observation of SEM (JEOL JSM-6300F) at an acceleration voltage of 10–15 kV and TEM (JEOL JEM-2010F).

3.9. Anti-oxidative stress test

Antioxidant enzymes of superoxidase dismutase (≥98%, Sigma-Aldrich) and catalase (Sigma-Aldrich) were mixed with cell suspension (*E. coli* and *S. aureus*). Different enzyme units (93.75, 187.5, 375, 750, 1500 U ml^{-1}) of superoxidase dismutase and catalase were used in this research. The experimental protocol followed the protocol described in Section 2.3.

3.10. Respiratory toxicity test

Lung function of Kunming male mice (5–6 weeks old, 22 ± 2 g; Hubei Province Experimental Animal Center, Wuhan, People's Republic of China) was evaluated in this research. All experimental procedures were approved by the Office of Scientific Research Management of Central China Normal University (approval ID: CCNU-IACUC-2016-003). Tests were carried out in sterilized animal house with negative pressure. The designed antimicrobial formulation was coated onto the inner wall of the exposure chamber. The coating volume per unit area is the same as was used in the antimicrobial test. Exposure time was 8 hours per day which followed the standard set by the American Conference of Governmental Industrial Hygienists (ACGIH). The exposure period was 7 days. Mice groups of clean gas and formaldehyde gas (3.0 mg m^{-3}) (HOPE-MED 8052 inhalation equipment, Hope-med Company, Tianjin, China) were applied for negative control and positive control. Leukocytes, neutrophils, and lymphocytes were collected in blood or bronchoalveolar lavage fluid. Cell numbers were counted using a blood cell analysis system (MTN-21, Matenu Technology Corp., Jinan, China). Lung function (Forced vital capacity, FVC) was measured using an AniRes2005 lung function system (Bestlab, version 2.0, China).

3.11. Lung histological assay

The left lungs of the mice were removed for histopathology slice preparation. All samples were fixed in 10% formalin solution (99%, Sigma-Aldrich) for 24 h at room temperature, cut into pieces, and the separate pieces stained with hematoxylin and eosin (H&E) following the procedure described by Liu *et al.*[75] Stained pieces were embedded in paraffin, sectioned into 10 μm slices, and observed using a DM 4000B microscope (Leica Microsystems GmbH, Wetzlar, Germany).

3.12. Statistical analysis

GraphPad Prism software was used for statistical analysis of the experimental data, and for graphing the results. All data are presented as the mean & standard deviation (S.D.). The presence of statistical differences between groups was determined by ANOVA. The method of least significant difference (LSD) was used to compare the effects between each exposure group and the control. $p < 0.05$ and $p < 0.01$ were considered significant.

4. Conclusions

A smart functional coating was synthesized to exhibit long-term "release-killing", "contact-killing" and "anti-adhesion" activity against bacteria, endospores and viruses. The coating was formulated from anti-pathogen micelles tethered with copper nanoparticles using a green synthesis method that used L-vitamin C. The micelles prevented the encapsulated ClO_2 from quickly evaporating, and also were active in sustained release-killing. The copper nanoparticles tethered to the micelle surface improved the micelle stability and contact-killing ability. To prepare copper nanoparticles in a green environment, we used ascorbic acid (Vitamin C) in our chemical reduction process to avoid toxicity. Ascorbic acid works both as a reducing and protecting agent, which makes the process economical, nontoxic and environmentally friendly. Finally, the applied polymers provided great anti-adhesive properties to our designed coatings. Hydrophilic PEO side-chains contributed to preventing bacterial attachment to the coating surface. Based on the evidence, pathogens are thought to be killed by bio-oxidation of the designed coating. Coating-released ClO_2 could oxidize the cell membrane and penetrate into the cell to oxidize macromolecules. In addition, copper is especially active in generating hydroxyl radicals in the presence of ascorbic acid. The designed coating displayed release-killing by a sustained release of aqueous ClO_2. Since aqueous ClO_2 can potentially evaporate (it exists as a gas at room temperature), we evaluated its toxicity towards the respiratory system. We found that the designed coating exhibited good respiratory biocompatibility. It means that the designed coating could effectively control ClO_2 release in a safe range while being sufficient to kill pathogens. This new anti-pathogen coating provides an additional measure of protection against the spread of diseases in high risk situations encountered in natural and manmade disasters, and during outbreaks of disease in either human or animal populations.

Conflicts of interest

The authors declare that they have no competing interests.

Acknowledgements

This work was supported by the National Natural Science Foundation of China (No. 21607117), the National Natural Science Foundation of China (No. 21577045) and the Foundation of Excellent Young Scholar of Wuhan Polytechnic University (No. 2018RZ01).

Notes and references

1 R. Rappuoli, M. Pizza, G. D. Giudice and E. D. Gregorio, *Proc. Natl. Acad. Sci. U. S. A.*, 2014, **111**, 12288–12293.
2 Z. Lin, Y. Li, M. Guo, T. Xu, C. Wang, M. Zhao, H. Wang, T. Chen and B. Zhu, *RSC Adv.*, 2017, **7**, 742–750.
3 B. J. Cowling, D. K. Ip, V. J. Fang, P. Suntarattiwong, S. J. Olsen and J. Levy, *Nat. Commun.*, 2013, **4**, 1935.
4 J. M. Read and M. J. Keeling, *Proc. Biol. Sci.*, 2003, **270**, 699–708.
5 C. P. McCoy, R. A. Craig, S. M. McGlinchey, L. Carson, D. S. Jones and S. P. Gorman, *Biomaterials*, 2012, **33**, 7952–7958.
6 A. Kramer, I. Schwebke and G. Kampf, *BMC Infect. Dis.*, 2006, **6**, 130.
7 K. K. Jefferson, *FEMS Microbiol. Lett.*, 2004, **236**, 163–173.
8 R. M. Donlan and J. W. Costerton, *Clin. Microbiol. Rev.*, 2002, **15**, 167–193.
9 K. E. Byers, L. J. Durbin, B. M. Simonton, A. M. Anglim, K. A. Adal and B. M. Farr, *Infect. Control Hosp. Epidemiol.*, 1998, **19**, 261–264.

10 J. S. Yang, H. C. Zheng, S. Y. Han, Z. D. Jiang and X. Chen, *RSC Adv.*, 2015, **5**, 2378–2382.
11 K. Vijayalakshmi and D. Sivaraj, *RSC Adv.*, 2016, **6**, 9663–9671.
12 Y. Wu, Y. T. Yang, H. Y. Liu, X. H. Yao, F. Leng, Y. Chen and W. Q. Tian, *RSC Adv.*, 2017, **7**, 18917–18925.
13 T. Tamanna, J. B. Bulitta, C. B. Landersdorfer, V. Cashin and A. Yu, *RSC Adv.*, 2015, **5**, 107839–107846.
14 M. S. Acevedoa, C. Puentesa and K. Carreño, *Int. Biodeterior. Biodegrad.*, 2013, **83**, 97–104.
15 M. R. Reithofer, A. Lakshmanan, A. T. Ping, J. M. Chin and C. A. Hauser, *Biomaterials*, 2014, **35**, 7535–7542.
16 Z. Li, D. Lee, X. Sheng, R. E. Cohen and M. F. Rubner, *Langmuir*, 2006, **22**, 9820–9823.
17 P. J. Rivero, A. Urrutia, J. Goicoechea, C. R. Zamarreño, F. J. Arregui and I. R. Matías, *Nanoscale Res. Lett.*, 2011, **6**, 305.
18 C. L. Chen, J. S. Makib and D. Rittschofc, *Int. Biodeterior. Biodegrad.*, 2013, **83**, 71–76.
19 X. Laloyaux, E. Fautre, T. Blin, V. Purohit, J. Leprince, T. Jouenne, A. M. Jonas and K. Glinel, *Adv. Mater.*, 2010, **22**, 5024–5028.
20 G. McDonnel and D. Russel, *Clin. Microbiol. Rev.*, 1999, **12**, 147–179.
21 J. Tsibouklis, M. Stone and A. A. Thorpe, *Biomaterials*, 1999, **20**, 1229–1235.
22 J. Israelachvili, *Proc. Natl. Acad. Sci. U. S. A.*, 1997, **24**, 8378–8379.
23 E. Lih, S. H. Oh, Y. K. Joung, J. H. Lee and D. K. Han, *Prog. Polym. Sci.*, 2015, **44**, 28–61.
24 N. J. Ragab-Depre, *Appl. Environ. Microbiol.*, 1982, **44**, 555–560.
25 A. T. Ficheux, L. Bonakdar, F. Leal-Calderon and J. Bibette, *Langmuir*, 1998, **14**, 2702–2706.
26 Y. Li, W. K. Leung, K. L. Yeung, P. S. Lau and J. K. Kwan, *Langmuir*, 2009, **25**, 13472–13480.
27 R. B. A. Kolsi, B. Gargouri, S. Sassi, D. Frikha, S. Lassoued and K. Belghith, *Lipids Health Dis.*, 2017, **16**, 252.
28 A. Khan, A. Rashid, R. Younas and R. Chong, *Int. Nano Lett.*, 2016, **6**, 21–26.
29 N. M. Zain, A. G. F. Stapley and G. Shama, *Carbohydr. Polym.*, 2014, **112**, 195–202.
30 K. R. Peddireddy, T. Nicolai, L. Benyahia and I. Capron, *ACS Macro Lett.*, 2016, **5**, 283–286.
31 J. Zhou, X. Y. Qiao, B. P. Binks, K. Sun, M. W. Bai, Y. L. Li and Y. Liu, *Langmuir*, 2011, **27**, 3308–3316.
32 K. H. Bae, S. H. Choi, S. Y. Park, Y. H. Lee and T. G. Park, *Langmuir*, 2006, **22**, 6380–6384.
33 S. Magdassi and N. Garti, *J. Controlled Release*, 1986, **3**, 273–277.
34 Y. Sela, S. Magdassi and N. J. Garti, *J. Controlled Release*, 1995, **33**, 1–12.
35 G. Gao, D. Lange, K. Hilpert, J. Kindrachuk and Y. Zou, *Biomaterials*, 2011, **32**, 3899–3909.
36 K. D. Xu, G. A. Mcfeters and P. S. Stewart, *Microbiology*, 2000, **146**, 547–549.
37 A. K. Muszanska, H. J. Busscher, A. Herrmann, H. C. van and W. Norde, *Biomaterials*, 2011, **32**, 6333–6341.
38 M. R. Nejadnik, H. C. van der Mei, W. Norde and H. J. Busscher, *Biomaterials*, 2008, **29**, 4117–4121.
39 M. R. Nejadnik, A. L. Olsson, P. K. Sharma, H. C. van der Mei, W. Norde and H. J. Busscher, *Langmuir*, 2009, **25**, 6245–6249.
40 M. Chen, Q. Yu and H. Sun, *Int. J. Mol. Sci.*, 2013, **14**, 18488–18501.
41 J. R. Morones, J. L. Elechiguerra and A. Camacho, *Nanotechnology*, 2005, **16**, 2346–2353.
42 E. N. Gkana, A. I. Doulgeraki, N. G. Chorianopoulos and G. E. Nychas, *Front. Microbiol.*, 2017, **8**, 1295.
43 D. Jasovský, J. Littmann, A. Zorzet and O. Cars, *Upsala J. Med. Sci.*, 2016, **121**, 159–164.
44 F. J. Schmitz, P. G. Higgins, S. Mayer, A. C. Fluit and A. Dalhoff, *Eur. J. Clin. Microbiol. Infect. Dis.*, 2002, **21**, 647–659.
45 C. F. Amabile-Cuevas, R. Pina-Zentella and M. E. Wah-Laborde, *Mutat. Res.*, 1991, **264**, 119–125.
46 Z. O. Alabi, K. D. Thomas, O. Ogunbona and I. A. Elegbe, *Afr. J. Med. Med. Sci.*, 1994, **23**, 143–146.
47 Z. Bai, D. E. Cristancho, A. A. Rachford, A. L. Reder, A. Williamson and A. L. Grzesiak, *J. Agric. Food Chem.*, 2016, **64**, 8647–8652.
48 N. J. Ragab-Depre, *Appl. Environ. Microbiol.*, 1982, **44**, 555–560.
49 P. J. Jansson, C. Lindqvist and T. Nordström, Iron prevents ascorbic acid (vitamin C) induced hydrogen peroxide accumulation in copper contaminated drinking water, *Free Radical Res.*, 2005, **39**, 1233–1239.
50 S. B. Nimse and D. Pal, *RSC Adv.*, 2015, **5**, 27986–28006.
51 K. Brawn and I. Fridovich, *Acta Physiol. Scand., Suppl.*, 1980, **492**, 9–18.
52 F. D'Agnillo and T. M. S. Chang, *Nat. Biotechnol.*, 1998, **16**, 667–671.
53 D. G. Bouzianas, *Trends Microbiol.*, 2009, **17**, 522–528.
54 R. V. Orr and L. R. Beuchat, *J. Food Prot.*, 2000, **63**, 1117.
55 J. B. Cross, R. P. Currier, D. J. Torraco, L. A. Vanderberg, G. L. Wagner and P. D. Gladen, *Appl. Environ. Microbiol.*, 2003, **69**, 2245–2252.
56 D. Rodríguez-Lázaro, N. Cook, F. M. Ruggeri, J. Sellwood, A. Nasser, M. S. Nascimento and W. H. van der Poel, *FEMS Microbiol. Rev.*, 2012, **36**, 786–814.
57 G. R. Taylor and M. Butler, *J. Hyg.*, 1982, **89**, 321–328.
58 L. Zimmerman, *J. Bacteriol.*, 1966, **91**, 1537–1542.
59 J. L. Sagripanti, L. B. Routson, A. C. Bonifacino and C. D. Lytle, *Antimicrob. Agents Chemother.*, 1997, **41**, 812–817.
60 L. Colobert, *Rev. Pathol. Gen. Physiol. Clin.*, 1962, **62**, 551–555.
61 N. Ogata, *J. Gen. Virol.*, 2012, **93**, 2558–2563.
62 S. N. Madhusudana, R. Shamsundar and S. Seetharaman, *Int. J. Infect. Dis.*, 2004, **8**, 21–25.
63 N. H. Loukili, N. Lemaitre, B. Guery, O. Gaillot, D. Chevalier and G. Mortuaire, *J. Infect. Prev.*, 2017, **18**, 78–83.
64 N. Ogata, M. Sakasegawa, T. Miura, T. Shibata, Y. Takigawa, K. Taura, K. Taguchi, K. Matsubara, K. Nakahara, D. Kato, K. Sogawa and H. Oka, *Pharmacology*, 2016, **97**, 301–306.

65 J. W. Yeap, S. Kaur, F. Lou, E. DiCaprio, M. Morgan, R. Linton and J. Li, *Appl. Environ. Microbiol.*, 2015, **82**, 116–123.
66 N. Ogata, M. Sakasegawa, T. Miura, T. Shibata and Y. Takigawa, *Pharmacology*, 2016, **97**, 301–306.
67 C. W. White and J. G. Martin, *Proc. Am. Thorac. Soc.*, 2010, **7**, 257–263.
68 A. A. Aksenov, A. Gojova, W. Zhao, J. T. Morgan, S. Sankaran, C. E. Sandrock and C. E. Davis, *ChemBioChem*, 2012, **13**, 1053–1059.
69 G. J. Guthrie, K. A. Charles, C. S. Roxburgh, P. G. Horgan, D. C. McMillan and S. J. Clarke, *Crit. Rev. Oncol. Hematol.*, 2013, **88**, 218–230.
70 H. Y. Reynolds, J. D. Fulmer, J. A. Kazmierowski, W. C. Roberts, M. M. Frank and R. G. Crystal, *J. Clin. Invest.*, 1977, **59**, 165–175.
71 H. Ranu, M. Wilde and B. Madden, *Ulster Med. J.*, 2011, **80**, 84–90.
72 Y. Q. Li, B. P. Bastakoti, V. Malgras, C. L. Li, J. Tang, J. H. Kim and Y. Yamauchi, *Angew. Chem., Int. Ed.*, 2015, **54**, 11073–11077.
73 Y. Li, B. P. Bastakoti, M. Imura, S. M. Hwang, Z. Sun, J. H. Kim, S. X. Dou and Y. Yamauchi, *Chem.–Eur. J.*, 2014, **20**, 6027–6032.
74 C. R. Gaush and T. F. Smith, *Appl. Microbiol.*, 1968, **16**, 588–594.
75 X. Liu, Y. Zhang, J. Li, D. Wang, Y. Wu and Y. Li, *Int. J. Nanomed.*, 2014, **11**, 823–839.